Magnetic properties and magnetocaloric effects in $Er_{1-x}Gd_xCoAl$ intermetallic compounds*

Gao Xin-Qiang(高新强)[a)b)], Mo Zhao-Jun(莫兆军)[a)b)], Shen Jun(沈 俊)[b)†], Li Ke(李 珂)[b)], Dai Wei(戴 巍)[b)], Wu Jian-Feng(吴剑峰)[b)], and Tang Cheng-Chun(唐成春)[a)‡]

[a)] *School of Material Science and Engineering, Hebei University of Technology, Tianjin* 300384, *China*

[b)] *Key Laboratory of Cryogenics, Technical Institute of Physics and Chemistry, Chinese Academy of Sciences, Beijing* 100190, *China*

(Received 16 October 2014; revised manuscript received 5 April 2015; published online 3 August 2015)

The magnetism and magnetocaloric effect in $Er_{1-x}Gd_xCoAl$ ($x = 0$, 0.1, 0.2, 0.4, 0.6, 0.8, 1) were investigated. The $Er_{1-x}Gd_xCoAl$ compounds were synthesized by arc melting. With the increasing Gd content, the Néel temperature (T_N) linearly increases from 14 K to 102 K, while the magnetic entropy change ($-\Delta S_M$) tends to decrease nonmonotonously. Under the field change from 0 T to 5 T, the $-\Delta S_M$ of the compounds with $x = 0.2$–1 are stable around 10 J/kg·K, then a cooling platform between 20 K and 100 K can be formed by combining these compounds. For $x = 0.6$, 0.8, 1.0, the compounds undergo two successive magnetic transitions, one antiferromagnetism to ferromagnetism and the other ferromagnetism to paramagnetism, with increasing temperature. The two continuous magnetic transitions in this series are advantageous to broaden the temperature span of half-peak width (δT) in the $-\Delta S_M$–T curve and improve the refrigeration capacity.

Keywords: mgnetocaloric effect, magnetic entropy change, magnetic phase transformation

PACS: 75.30.Sg, 65.40.gd, 75.30.Kz **DOI:** 10.1088/1674-1056/24/9/097502

1. Introduction

Magnetic refrigeration is a potential cooling technology due to its higher energy efficiency and lower environmental impact than the conventional vapor compression refrigeration.[1] The feasibility of applying this technology highly depends on the design and synthesis of suitable magnetic cooling materials. For a long time, looking for a high magnetic entropy change ($-\Delta S_M$) was regarded as the primary task.[2–4] A large number of materials with first-order magnetic transition, such as $LaFe_{13-x}Si_x$,[5–7] $MnAs_{1-x}Sb_x$,[8,9] $MnFeP_xAs_{1-x}$,[10–12] and $Mn_{1-x}Fe_xAs$,[13] have been found to exhibit the giant magnetocaloric effect (MCE). However, the magnetic entropy change is not the only parameter to evaluate the cooling capacity of a refrigerant material. The refrigerant capacity (RC), $RC = \int_{T_1}^{T_2} |\Delta S_M| dT$, is considered as another important parameter of a potential magnetic refrigerant.[5,14] It is a measure of the amount of heat transfer between the cold and hot reservoirs in an ideal refrigeration cycle. For a potential refrigerant with large RC, not only the large magnetic entropy is required, but also the wide half-peak width of the refrigerant temperature region is necessary.

It has been reported that the RCoAl (R = Gd, Tb, Dy, Ho) compound shows a large magnetic entropy change in a wide temperature span near the transition temperature.[15] For example, in the soft magnetic GdCoAl compound, a table-like behavior from 70 K to 105 K was found in the temperature dependence of $-\Delta S_M$. These compounds crystallize in the $MgZn_2$-type hexagonal structure with ordered temperatures in the range from 10 K to 100 K. Especially, the GdCoAl compound has a ferromagnetic transition at 100 K.[16] It crystallizes in the hexagonal $MgZn_2$ structure (space group $P63/mmc$), which is a close-packed laves phase. The absence of magnetic moment on Co was reported despite the fact that the 3d shell of Co is not completely filled.[17] This means that only the S-state Gd^{3+} ions contribute to the magnetic properties of GdCoAl. In other derived compounds such as Gd2Co2Al and $GdCo_{0.74}Al_{1.26}$, the metamagnetic transition of ferromagnetic transition and the glassy phase near 80 K result in the occurrence of a table-like magnetocaloric effect with a magnitude of −7 J/kg·K over the temperature range from 47.5 K to 77.5 K for a magnetic field variation from 0 T to 5 T.[18] In this work, we introduce continuous magnetic transitions in the compounds by the substitution of different rare earth elements, which broaden the $-\Delta S_M$ temperature span. The polycrystalline $Er_{1-x}Gd_xCoAl$ ($x = 0$–1) compounds are synthesized and their magnetic properties and MCE properties are investigated. With the substitution of Gd for Er, T_N increases and $-\Delta S_M$ exhibits a decreasing trend, however, RC is improved, which originates from the broadened temperature span (δT) in the $-\Delta S_M$–T curve.

2. Experiments

The polycrystalline samples of $Er_{1-x}Gd_xCoAl$ ($x = 0$, 0.2, 0.4, 0.6, 0.8, 1) were synthesized by arc melting of sto-

*Project supported by the National Natural Science Foundation of China (Grant Nos. 51322605 and 51271192).

†Corresponding author. E-mail: jshen@mail.ipc.ac.cn

‡Corresponding author. E-mail: tangcc@hebut.edu.cn

© 2015 Chinese Physical Society and IOP Publishing Ltd

ichiometric amounts of the elements with purity 99.9 wt.% in a water-cooled copper hearth under a purified argon atmosphere. The weight of rare earth metal R was 3% more than the theoretical value in order to compensate the loss. The samples were remelted three times to ensure the homogeneity. The samples were annealed at 1123 K for 10 days in a quartz tube with a high vacuum, and a subsequent quenching to room temperature was performed to obtain crystalline samples. Powder x-ray diffraction (XRD) measurements were performed at room temperature by using Cu $K\alpha$ radiation to identify the crystal structure. The x-ray powder diffraction patterns showed that the $Er_{1-x}Gd_xCoAl$ ($x = 0$, 0.2, 0.4, 0.6, 0.8, 1) compounds crystallize in the $MgZn_2$-type hexagonal structure and no impurity phases were detected. Magnetization measurements were carried out by employing a commercial superconducting quantum interference device (SQUID) magnetometer, model MPMS-7 from Quantum Design Inc.

3. Results and discussion

Figure 1 shows the temperature dependences of magnetization for the $Er_{1-x}Gd_xCoAl$ ($x = 0$, 0.2, 0.4, 0.6, 0.8, 1) compounds under zero-field-cooling (ZFC) and field-cooling (FC) with a magnetic field of 0.01 T. The ZFC curves show that the transition temperature increases from 14 K to 102 K as the content of Gd increases, as shown in Fig. 2. With increasing temperature, ErCoAl exhibits an AFM–PM magnetic transition at $T_N = 14$ K (Fig. 1(a)), this is similar to the cases of $x = 0.2$, 0.4 (Figs. 1(b) and 1(c)). With the substitution of Gd for Er, the compound with $x = 0.6$ exhibits two successive magnetic transitions, i.e., a transition from AFM to FM at $T_N = 53$ K and a transition from FM to PM at $T_C = 58$ K (Fig. 1(d)). From Fig. 1(d), one can see that the magnetization increases rapidly below 11 K and slowly in the range of 11–53 K upon temperature increasing, indicating the occurrence of magnetic phase separation of FM and AFM at low temperature. As shown in Fig. 1(f), no thermal hysteresis is observed for the GdCoAl compound, while a bifurcation is observed between ZFC and FC curves below T_C which should be related to the domain effect during the field cooling process. A small kink is observed around 117 K in the GdCoAl compound, which may be caused by the partial FM clusters.

The magnetization data above 150 K of all samples can be well fitted using the Curie–Weiss law with the expression $\chi^{-1} = (T - \theta)/C$, where θ denotes the Weiss constant and C is the Curie constant. Figure 2 shows the Gd doping x dependence of Curie temperature T_{ord} and Curie–Weiss temperature T_{CW} . One can see that both the Curie–Weiss temperature and the ordered temperature increase with increasing x, suggesting an increase of the ferromagnetic interaction due to the contribution from the Gd sublattice. Based on the formula $\mu_{eff} = (3k_BC/N_A)^{1/2}$ (k_B and N_A being the Boltzmann constant and the Avogadro constant), the paramagnetic effective magnetic moment μ_{eff} can also be determined. The μ_{eff} seems to show an increasing trend with x to 0.6 then starts to drop, while the theoretical value obtained according to the formula $P_{eff} = \sqrt{(x \times 7.9)^2 + [(1-x) \times 9.6]^2 + 6.63^2}\mu_B$ ($6.63\mu_B$, $9.6\mu_B$, and $7.9\mu_B$ for Co, Er, and Gd atoms, respectively) shows an opposite trend. The experimental values of μ_{eff} for $x = 0$, 0.2, 0.8, 1.0 are lower than the theoretical ones, which must originate from the short-range interaction in the paramagnetic region. For the compounds of $x = 0.4$ and 0.6, the experimental values of μ_{eff} are higher than the theoretical ones, which might indicate that the coupling interaction among the magnetic atoms near $x = 0.5$ is weaker than the theoretical predication based on the formula.

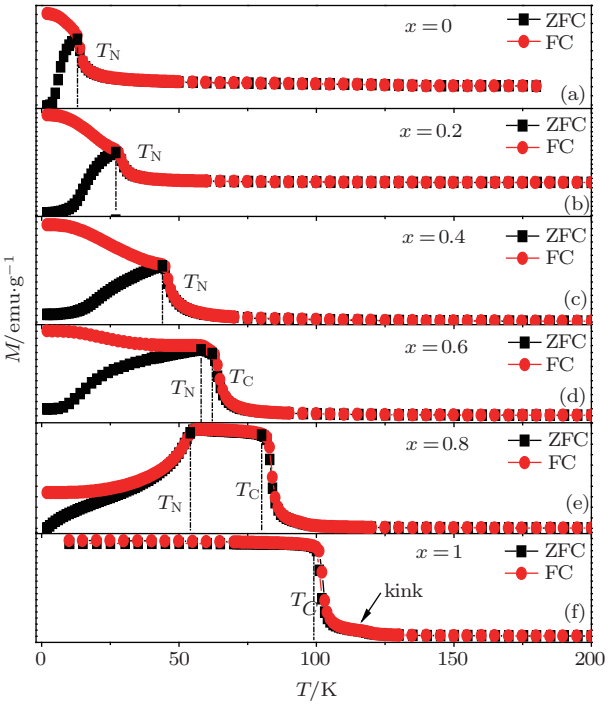


Fig. 1. (color online) Temperature dependences of magnetization for $Er_{1-x}Gd_xCoAl$ ((a) $x = 0$, (b) $x = 0.2$, (c) $x = 0.4$, (d) $x = 0.6$, (e) $x = 0.8$, (f) $x = 1$) compounds under ZFC and FC with a magnetic field of 0.01 T.

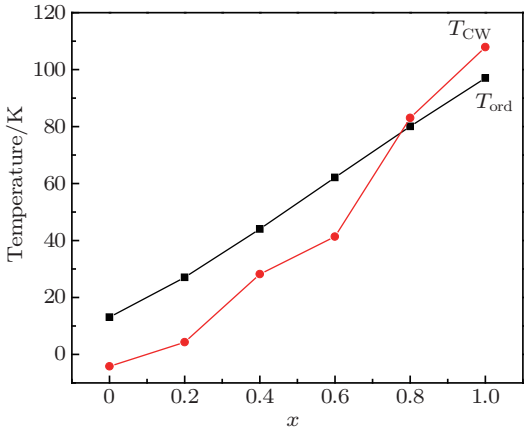


Fig. 2. (color online) The x dependences of Curie temperature T_{ord} and Curie–Weiss temperature T_{CW}.

Magnetization isotherms of the $Er_{1-x}Gd_xCoAl$ ($x = 0$, 0.2, 0.4, 0.6, 0.8, 1) compounds were measured at different low temperatures under applied fields up to 1.5 T, as shown in Fig. 3. All the compounds show antiferromagnetic like characteristics since the saturation is not reached at 5 T except GdCoAl, which shows a ferromagnetic feature. As shown in Fig. 3(f), the magnetization increases linearly with the increase of the magnetic field in the low field range, then the magnetization increases rapidly with increasing magnetic field and saturates quickly. It confirms the field-induced metamagnetic transition from AFM to FM state and finally the FM state is obtained as the magnetic field approaches ~ 1 T. The magnetic moment per formula M_s at 5 T and 5 K is calculated, which increases with the Gd content x. Theoretically, the magnetic moment of Er is larger than that of Gd and the total magnetic moment should be reduced by the gradual replacement of Gd for Er. However, the total magnetic moment is increased at low temperature, which implies that the introduction of Gd at the Er position brings about the magnetic moment arranged partially parallel with Er or the induced crystal field change results in Co spin moment reorientation. At the same time, the exchange of AFM or the magnetic anisotropy may be reduced as well. For example, the element Er was used to cancel the anisotropy of Dy, since the Stevens factors of Dy and Er have opposite signs.[19] Therefore, the magnetic property is changed and the total magnetic moment exhibits a complex phenomenon either in high or low temperatures with the substitution of Gd for Er.

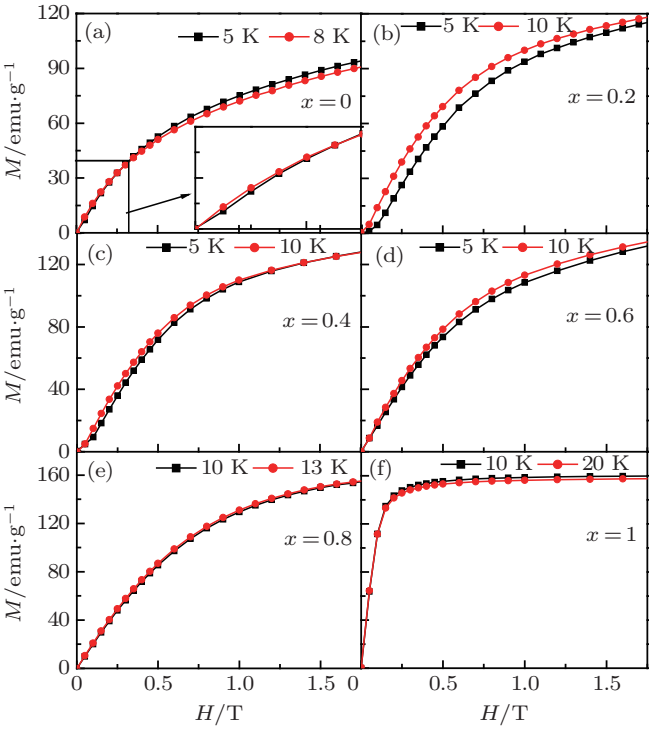


Fig. 3. (color online) Magnetization isotherms of $Er_{1-x}Gd_xCoAl$ ($x = 0$, 0.2, 0.4, 0.6, 0.8, 1) compounds measured at low temperature.

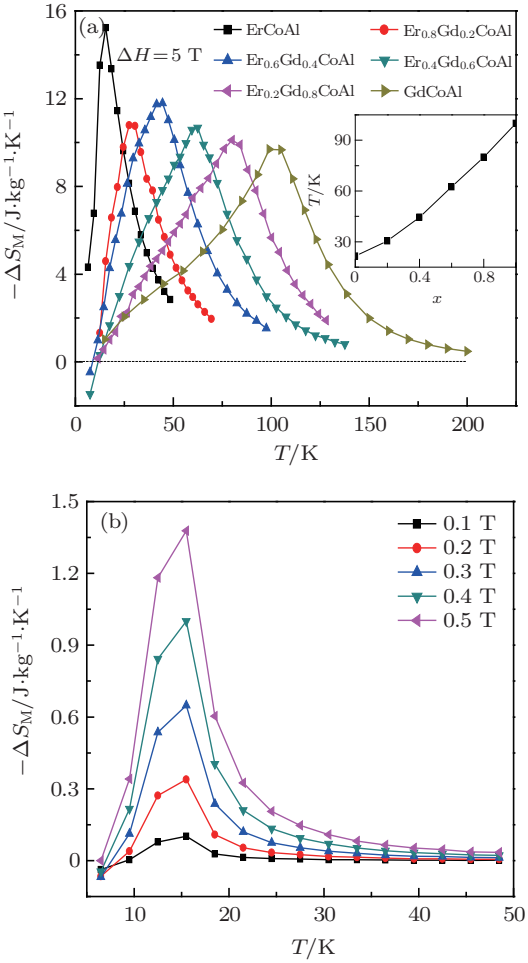


Fig. 4. (color online) (a) The magnetic entropy change as a function of temperature for the $Er_{1-x}Gd_xCoAl$ ($x = 0$, 0.2, 0.4, 0.6, 0.8, 1) compounds under 0–5 T. Inset: the content of Gd as a function of the temperature corresponding to $-\Delta S_M^{max}$. (b) Temperature dependence of the magnetic entropy change of the ErCoAl compound measured in a low magnetic field.

The isothermal magnetic entropy changes $-\Delta S_M$ of $Er_{1-x}Gd_xCoAl$ ($x = 0$–1) are obtained from the experimental isothermal magnetization data by using the Maxwell relation $\Delta S(T,H) = \int_0^H (\partial M/\partial T)_H \mathrm{d}H$. Figure 4(a) shows the temperature dependences of $-\Delta S_M$ for the magnetic field change of 5 T. The maximum magnetic entropy changes ($-\Delta S_M^{max}$) are 15.2 J/kg·K, 10.8 J/kg·K, 11.8 J/kg·K, 10.7 J/kg·K, 10.1 J/kg·K, and 9.7 J/kg·K for $x = 0$, 0.2, 0.4, 0.6, 0.8, 1.0, respectively. The $-\Delta S_M^{max}$ are all around 10.5 J/kg·K for the $Er_{1-x}Gd_xCoAl$ ($x = 0.2$–1) compounds with the corresponding temperature in the range from 20 K to 100 K. As shown in the inset of Fig. 4(a), the content of Gd as a function of the corresponding temperature of $-\Delta S_M^{max}$ exhibits a linear relationship, and the value of $-\Delta S_M^{max}$ shows a monotonously decreasing trend with x. The temperature span between two peaks is about 15 K with $\Delta x = 0.2$, and the small temperature span is conducive to forming a refrigeration platform. A great refrigeration platform in the temperature range from 20 K to 100 K can be obtained by the combination of these materials, which is very useful in the refrigerant application. In addi-

tion, the negative values of $-\Delta S_M$ are often observed below the Néel temperature. If the field induced AFM–FM transition exists, the $-\Delta S_M$ is always negative below the critical field.[20] It is obvious that the $Er_{0.4}Gd_{0.6}CoAl$ and $Er_{0.2}Gd_{0.8}CoAl$ compounds show negative $-\Delta S_M$ at low temperatures, but other samples only have negative $-\Delta S_M$ at low field and low temperature. For example, the $-\Delta S_M$ of the ErCoAl compound is negative under a magnetic field below 0.4 T at 6.5 K, as shown in Fig. 4(b).

As described above, the compounds with $x = 0.6$ and 0.8 exhibit two successive magnetic transitions as shown in Figs. 1(d) and 1(e), respectively. However, only one peak in the $-\Delta S_M$–T curve is observed in Fig. 4. To explain this phenomenon, the magnetic entropy changes as a function of temperature for the $Er_{0.4}Gd_{0.6}CoAl$ and $Er_{0.2}Gd_{0.8}CoAl$ compounds under low magnetic field are shown in Fig. 5. Two peaks are observed under low magnetic field (0.1–0.5 T) for $Er_{0.2}Gd_{0.8}CoAl$, which correspond to the two magnetic transitions. The $-\Delta S_M$ is mainly caused by the FM–PM transition, whereas the AFM–FM transition contributes to the half maximum of the peak width of $-\Delta S_M$. Meanwhile, with increasing magnetic field (Figs. 5(a) and 5(b)), the contribution to $-\Delta S_M$ from the FM–PM transition sharply increases, while that from the AFM–FM transition increases gently. With increasing the Gd content, the temperature span is increased due to the improvement of the AFM–FM transition upon warming. A slight depression of $-\Delta S_M$ seems to be responsible for the broadened temperature span with increasing x.

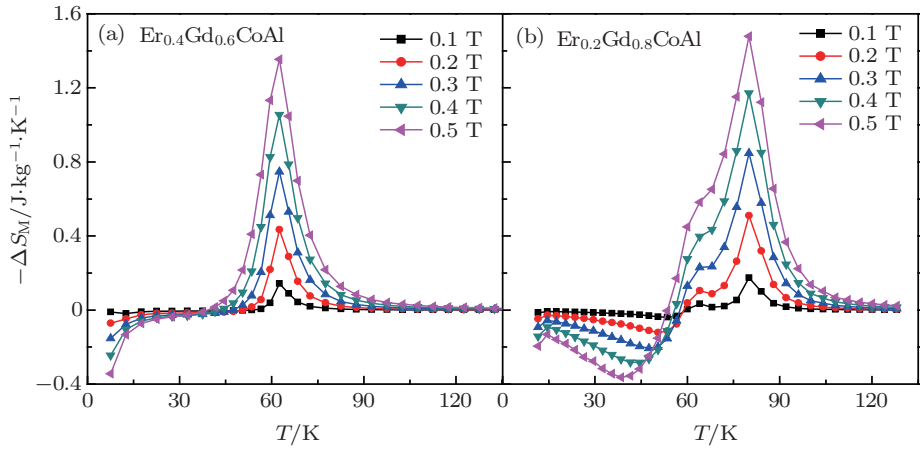


Fig. 5. (color online) Temperature dependences of magnetic entropy change in $Er_{0.4}Gd_{0.6}CoAl$ and $Er_{0.2}Gd_{0.8}CoAl$ with different magnetic field changes.

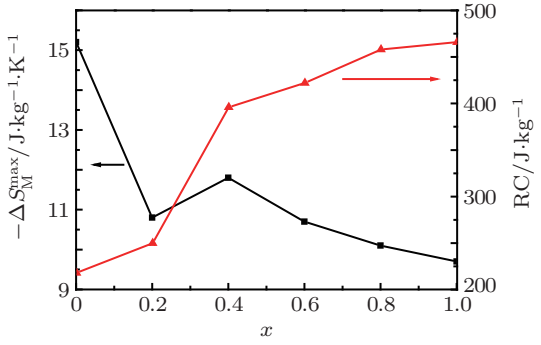


Fig. 6. (color online) The maximum entropy change and refrigeration capacity as a function of Gd content x.

The RC is considered to be an important parameter of a potential magnetic refrigerant. The RC is a measure of how much heat could be transferred between the hot and cold reservoirs in an ideal refrigerant cycle and a large RC is desirable. The RC is calculated by numerically integrating the area under the $-\Delta S_M$–T curve, $RC = \int_{T_1}^{T_2} |\Delta S_M| dT$, where T_1 and T_2 are the temperatures at half maximum of the peak. Figure 6 shows $-\Delta S_M^{max}$ and RC as a function of the Gd content x. With increasing x, the $-\Delta S_M^{max}$ exhibits a decreased trend while the RC increases, which is similar to the result of the $Er_{3-x}Gd_xCo$ compounds.[21] We can also conclude that the FM–PM transition is the main contribution to increasing the RC of $Er_{1-x}Gd_xCoAl$.

4. Conclusion

The magnetic and magnetocaloric properties of the $Er_{1-x}Gd_xCoAl$ ($x = 0$, 0.1, 0.2, 0.4, 0.6, 0.8, 1) compounds were investigated. The temperature dependence of magnetization showed that the introduction of Gd increases the magnetic transition temperature from 14 K to 102 K. The $-\Delta S_M^{max}$ of the $Er_{1-x}Gd_xCoAl$ ($x = 0$–1) compounds with $x = 0$, 0.2, 0.4, 0.6, 0.8, 1.0 under the magnetic field change of 5 T are 15.2 J/kg·K, 10.8 J/kg·K, 11.8 J/kg·K, 10.7 J/kg·K, 10.1 J/kg·K, and 9.7 J/kg·K, respectively. For the compounds with $x = 0.2$–1.0, the $-\Delta S_M$ are all around 10.5 J/kg·K, thus a refrigeration platform from 20 K to 100 K can be formed. The compounds show two successive magnetic transitions for

$x = 0.6$ and 0.8. With the increase of the Gd content, the $-\Delta S_{\mathrm{M}}^{\max}$ is decreased monotonously, whereas the RC is improved due to the broadened δT.

References

[1] Jia L, Sun J R, Zhang H W, Hu F X, Dong C and Shen B G 2006 *J. Phys.: Condens. Mater* **18** 9999

[2] Dagula W, Tegus O, Li X W, Song L, Brück E, Cam Thanh D T, de Boer F R and Buschow K H J 2006 *J. Appl. Phys*. **99** 08Q105

[3] Phan M H, Tian S B, Hoang D Q, Yu S C, Nguyen C and Ulyanov A N 2003 *J. Magn. Magn. Mater.* **258–259** 309

[4] Zhang H, Shen B G, Xu Z Y, Chen J, Shen J, Hu F X and Sun J R 2011 *J. Alloys Compd.* **509** 2602

[5] Hu F X, Shen B G, Sun J R and Zhang X X 2000 *Chin. Phys.* **9** 550

[6] Shen J, Gao B, Yan L Q, Li Y X, Zhang H W, Hu F X and Sun J R 2007 *Chin. Phys.* **16** 3848.

[7] Hu F X, Shen B G, Sun J R, Cheng Z H, Rao G H and Zhang X X 2001 *Appl. Phys. Lett.* **78** 3675

[8] Wada H and Tanabe Y 2001 *Appl. Phys. Lett.* **79** 3302

[9] Tegus O, Brück E, Buschow K H J and de Boer F R 2002 *Nature* **415** 150

[10] Tegus O, Bao L H, and Song L 2013 *Chin. Phys. B* **22** 037506

[11] Geng Y X, Tegus O and Bi L G 2012 *Chin. Phys. B* **21** 037504

[12] Brück E, Ilyn M, Tishin A M and Tegus O 2005 *J. Magn. Magn. Mater.* **290–291** 8

[13] Balli M, Fruchart D, Gignoux D and Zach R 2009 *Appl. Phys. Lett.* **95** 072509

[14] Shen B G, Sun J R, Hu F X, Zhang H W and Cheng Z H 2009 *Adv. Mater.* **21** 4545

[15] Zhang X X, Wang F W and Wen G H 2001 *J. Phys.: Condens. Matter* **13** L747

[16] Jarosz J, Talik E, Mydlarz T, Kusz J, Bohm H and Winiarski A 2000 *J. Magn. Magn. Mater.* **208** 169

[17] Chiu L B, Elliston P R, Stewart A M, Taylor K N R and Issa M A A 1980 *J. Phys. F* **10** 2297

[18] Fu H, Ma Z, Zhang X J, Wang D H, Teng B H and Agurgo Balfour E 2014 *Appl. Phys. Lett.* **104** 072401

[19] O'Handley R C 2000 *Modern Magnetic Materials—Principles and Applications* (New York: Wiley) p. 202

[20] Yan L Q, Chun S H, Sun Y, Shin K W, Jeon B G, Shen S P and Kim K H 2013 *J. Phys.: Condens. Matter* **25** 256006

[21] Mo Z J, Shen J, Yan L Q, Wu J F, Tang C C and Shen B G 2013 *J. Appl. Phys.* **113** 033908